US 20250259304A1

(19) United States
(12) Patent Application Publication
UEDA et al.
(10) Pub. No.: US 2025/0259304 A1
(43) Pub. Date: Aug. 14, 2025

(54) **PROGRAM FOR INDICATING HUNNER LESION, LEARNED MODEL, AND METHOD FOR GENERATING SAME**

(71) Applicant: **TOMO CO., LTD.**, Kyoto-shi (JP)

(72) Inventors: **Tomohiro UEDA**, Kyoto-shi (JP); **Andrey Grushnikov**, Tokyo (JP)

(21) Appl. No.: **19/195,939**

(22) Filed: **May 1, 2025**

Related U.S. Application Data

(63) Continuation of application No. 17/818,853, filed on Aug. 10, 2022, now Pat. No. 12,315,150, which is a continuation of application No. PCT/JP2021/043293, filed on Nov. 25, 2021.

(30) **Foreign Application Priority Data**

Nov. 25, 2020 (JP) 2020-195447

Publication Classification

(51) **Int. Cl.**
G06T 7/00 (2017.01)
G06T 7/70 (2017.01)

(52) **U.S. Cl.**
CPC ***G06T 7/0012*** (2013.01); ***G06T 7/70*** (2017.01); *G06T 2207/10068* (2013.01); *G06T 2207/20081* (2013.01); *G06T 2207/20084* (2013.01); *G06T 2207/30096* (2013.01)

(57) **ABSTRACT**

The present disclosure relates to a method for generating a learning model, a learned model, a program, and a controller of a bladder endoscope in which the program or the model is recorded. The method including: acquiring, as teaching data, endoscope image data on a Hunner lesion in a bladder; and generating the learning model by using the teaching data such that a bladder endoscope image serves as an input and the position indication of a Hunner lesion in the bladder endoscope image serves as an output. The program causing a computer to perform acquiring endoscope image data on a Hunner lesion in a bladder, inputting a target bladder endoscope image to a learning model in which a bladder endoscope image serves as an input and position-indication data on a Hunner lesion in an endoscope image serves as an output, and outputting the position indication of the Hunner lesion.

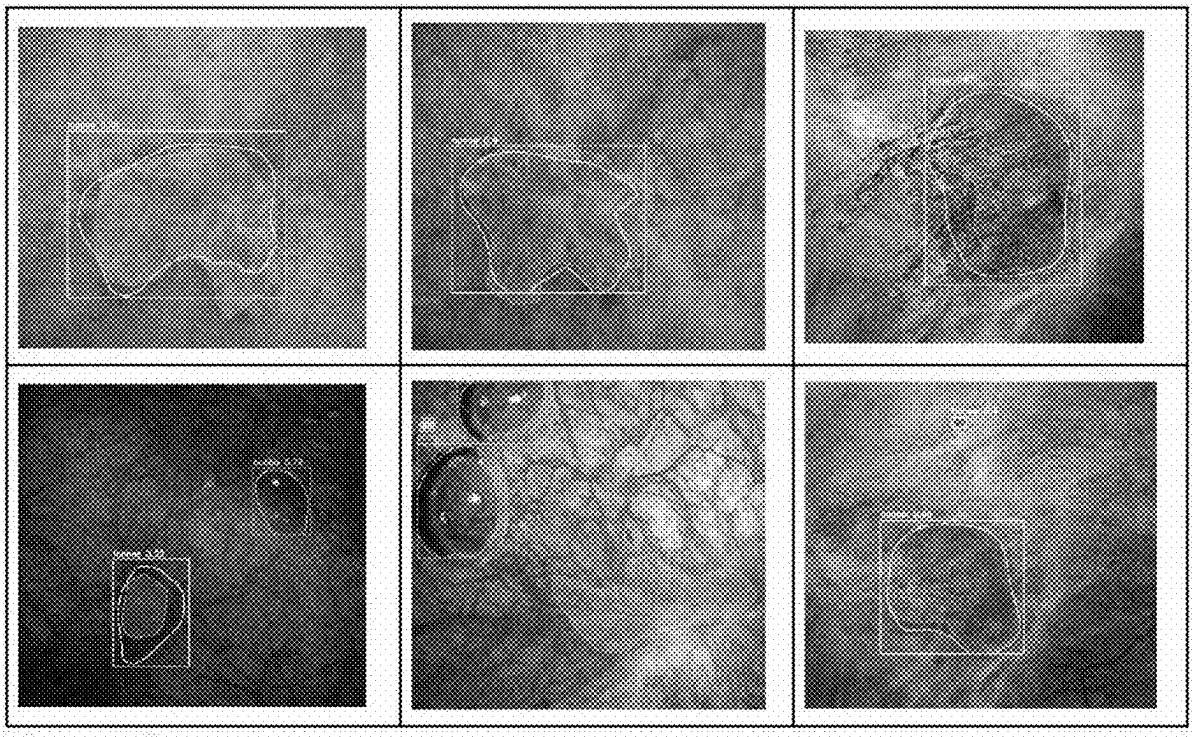

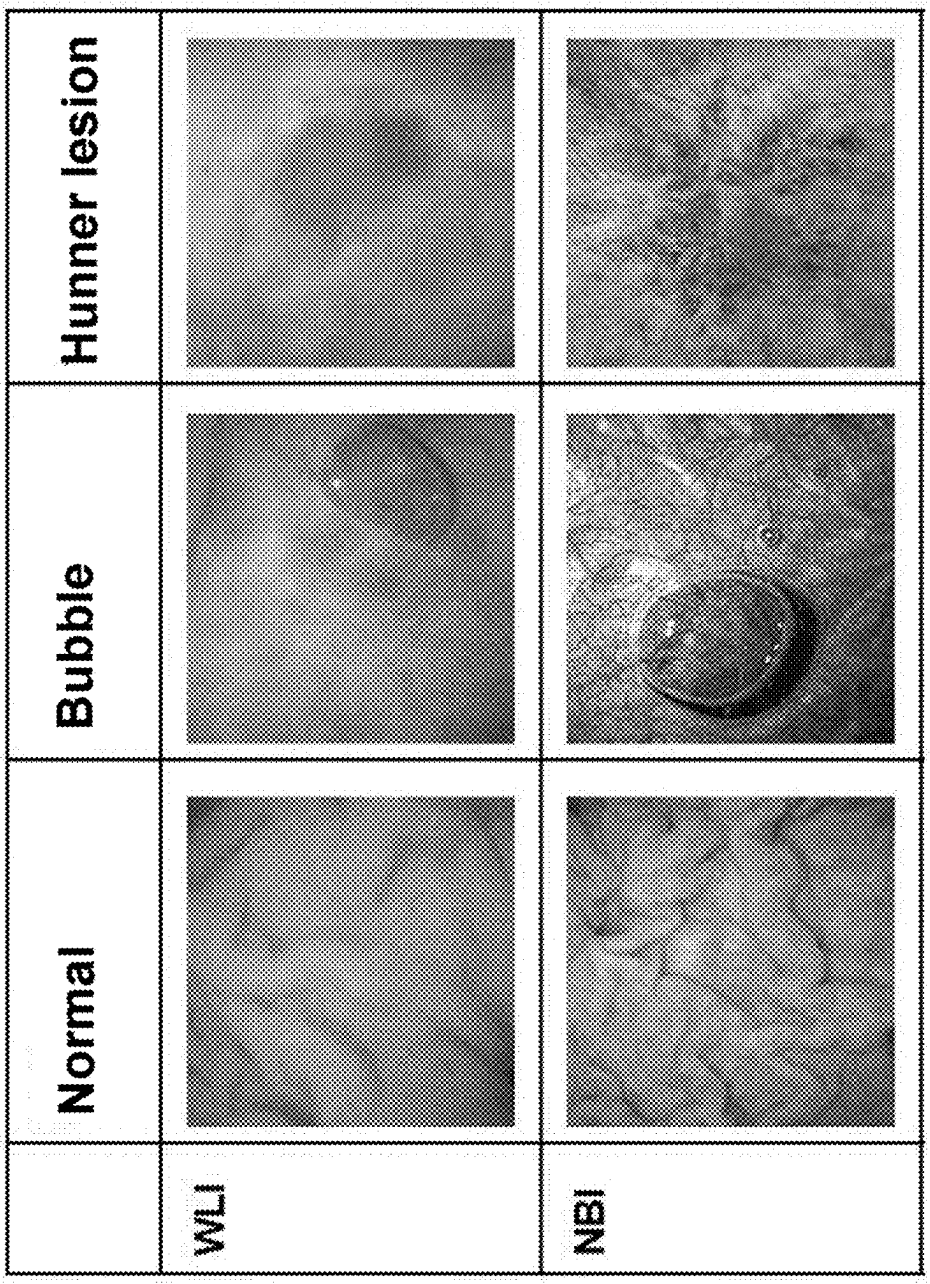

FIG. 1

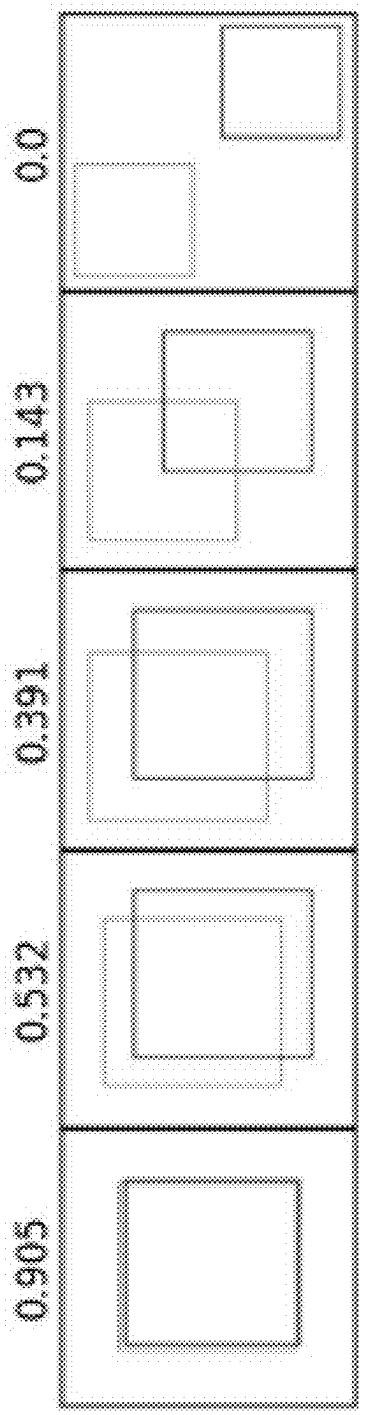

FIG. 2

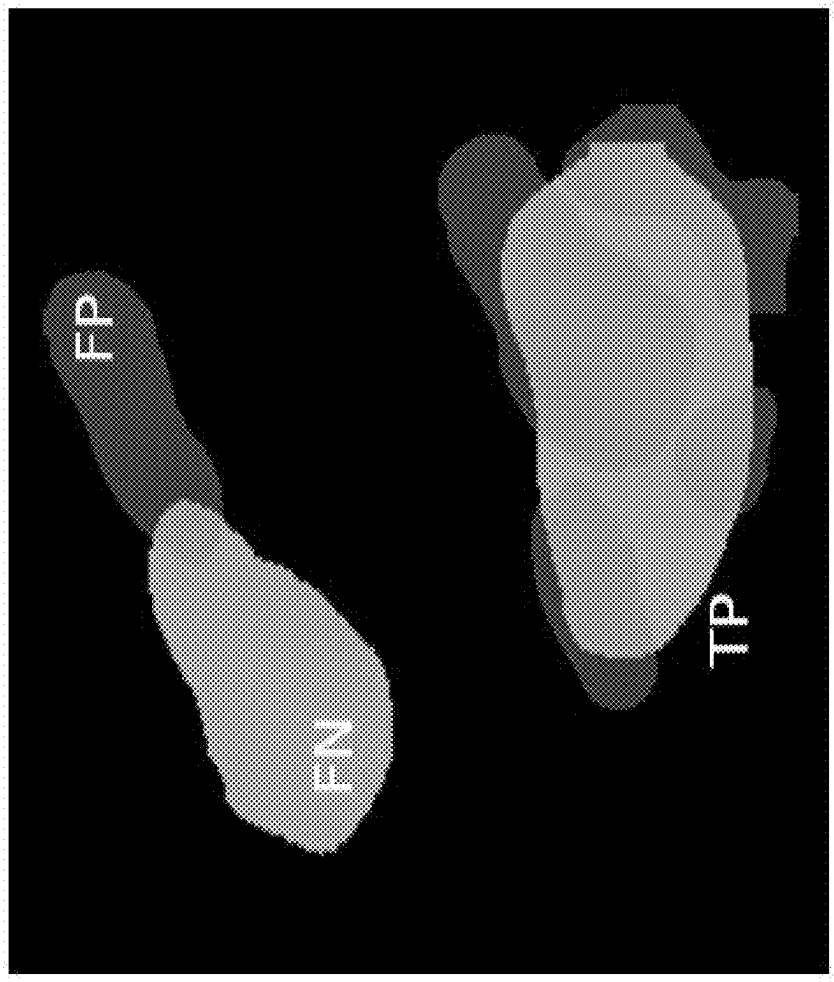

FIG. 3

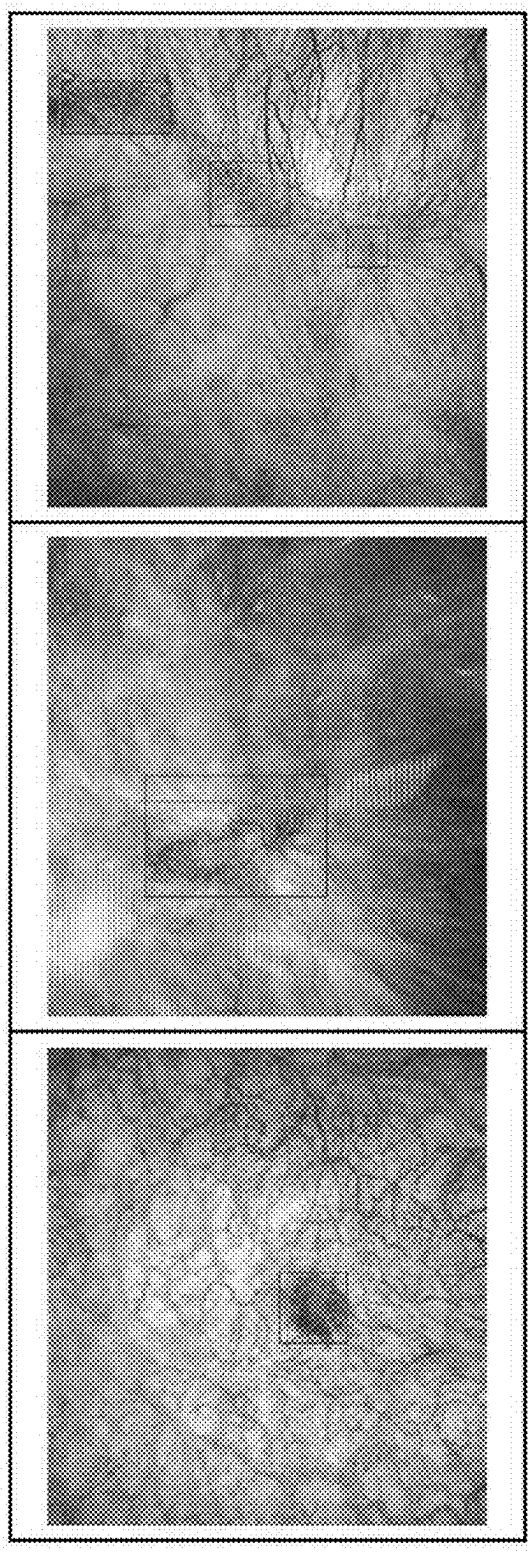

FIG. 4

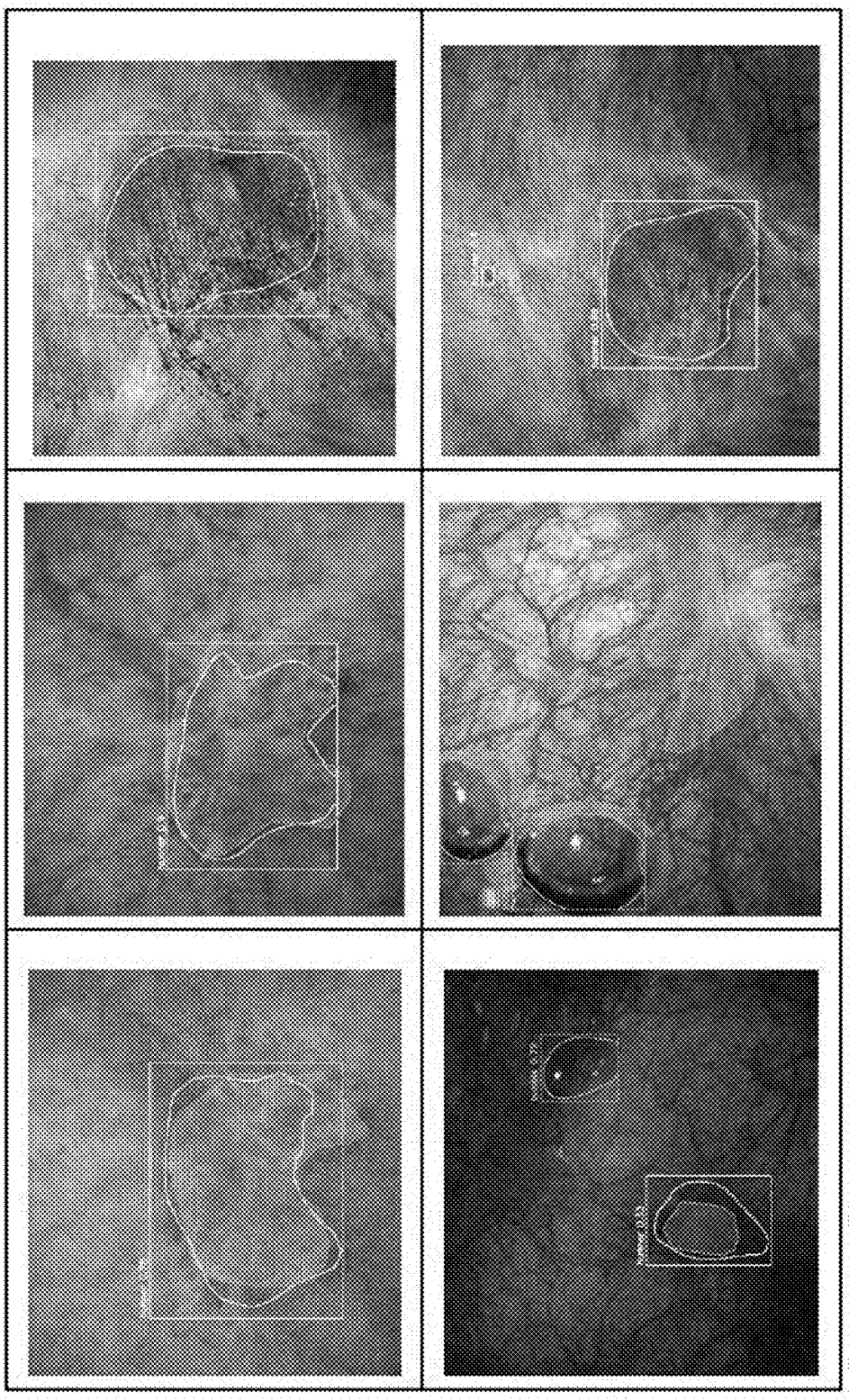

FIG. 5

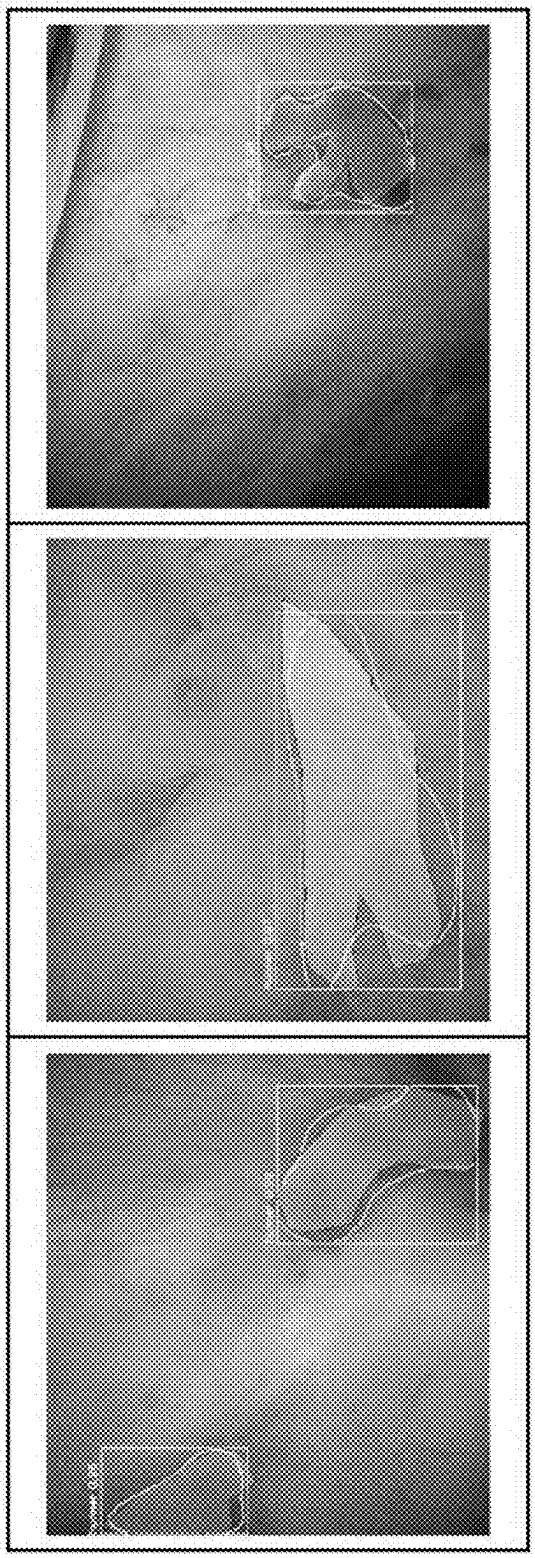

FIG. 6

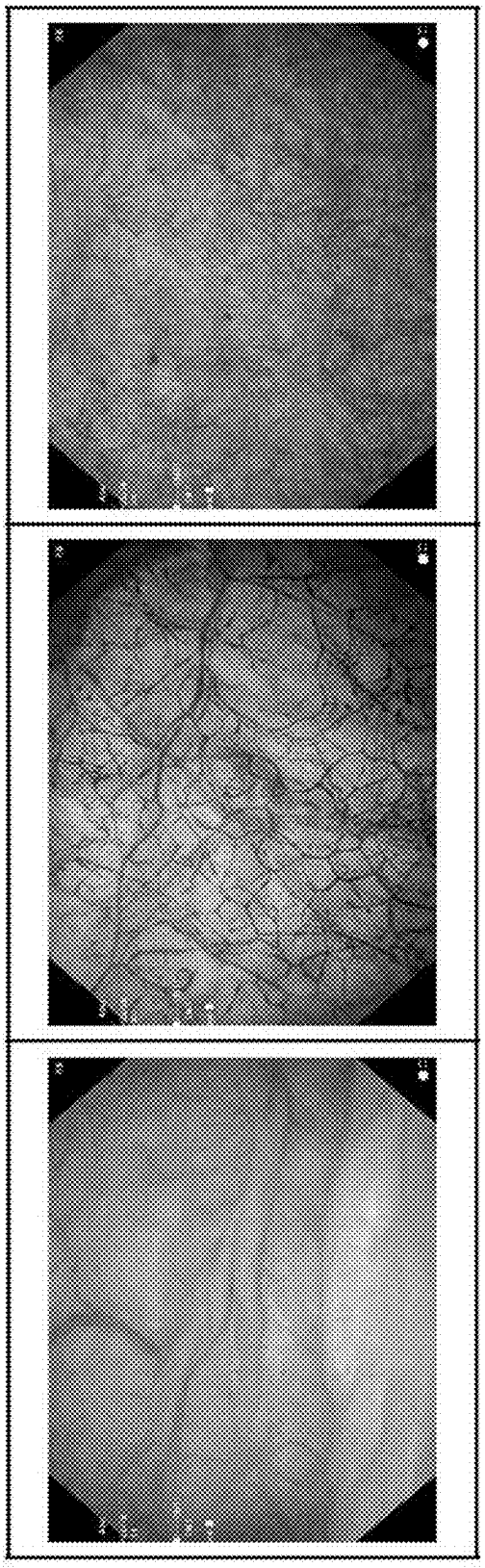

FIG. 7

PROGRAM FOR INDICATING HUNNER LESION, LEARNED MODEL, AND METHOD FOR GENERATING SAME

CROSS-REFERENCE TO RELATED APPLICATIONS

[0001] The present application is a continuation application of U.S. patent application Ser. No. 17/818,853, filed on Aug. 10, 2022 and entitled "PROGRAM FOR INDICATING HUNNER LESION, LEARNED MODEL, AND METHOD FOR GENERATING SAME," which is a continuation application of International Patent Application No. PCT/JP2021/043293 filed on Nov. 25, 2021, which claims priority to Japanese Patent Application No. JP2020-195447, filed on Nov. 25, 2020, the entire disclosures of which are incorporated herein by reference.

TECHNICAL FIELD

[0002] The present invention relates to a program useful for indicating a Hunner lesion. More specifically, the present invention relates to a program for indicating a target Hunner lesion, a learned model, and a method for generating the same in the field of bladder abnormalities, in particular, interstitial cystitis.

BACKGROUND

[0003] Interstitial cystitis is a chronic disease that causes symptoms such as frequent urination, urinary urgency, and cystalgia or discomfort with bladder fullness. A seriously ill patient may urinate 60 times a day, which causes considerable influence and results in difficulty in daily life. Women are more likely to develop interstitial cystitis men. Among about 1.3 million patients of interstitial cystitis in the U.S., at least one million patients are female. Although epidemiological surveys have been frequently conducted, the cause of the disease has not been discovered yet. Furthermore, the definitions, criteria, and expressions of "interstitial cystitis" vary among countries and regions. Thus, a description of "interstitial cystitis" in the present application also includes the concepts of cystalgia and overactive bladder pains.

[0004] The criteria of case collection study (Interstitial Cystitis Data Base; ICDB) 18) in the U.S. reflect criteria routinely used for interstitial cystitis in the U.S. In the criteria, cystoscopic findings are not preconditions. Moreover, NIDDK (National Institute of Diabetes and Digestive and Kidney Diseases) provides criteria that have been frequently cited. However, the criteria are used for strictly selecting cases during study. The criteria require cystoscopic findings and thus are more strictly defined. Some reports show that only less than half of patients diagnosed as interstitial cystitis by ICDB criteria meet the criteria of NIDDK.

[0005] As a characteristic of interstitial cystitis, the types of interstitial cystitis are broadly divided into a Hunner type having Hunner lesions and a non-Hunner type having no Hunner lesions. Hunner lesions are unique rubefacient mucous membranes having no normal capillary structures. Pathologically, epitheliums frequently fall off (erosion), and neovascularization and clustered inflammatory cells are found in submucosa. The Hunner type endoscopically and pathologically has definite abnormal findings. The Hunner type is a unique rubefacient mucous membrane having no normal capillary structures. As described above, any international criteria have not been established, and thus a Hunner lesion may be referred to as a Hunner's ulcer or may be simply referred to as an ulcer depending upon the region.

[0006] The Hunner type is more likely to cause serious conditions and thus requires correct diagnoses and treatments at an earlier stage. However, as described above, the presence or absence of a Hunner lesion is not defined as a requirement of the diagnosis of interstitial cystitis in some regions. Since the definition of global standards and criteria have not been established yet, only a few doctors can carry out diagnosis of interstitial cystitis and Hunner lesions with correct knowledge. Hence, even if U.S. Pat. No. 8,010,185 about the diagnosis of interstitial cystitis has been disclosed by Tomohiro Ueda, one of the inventors of the present invention, potential patients are missed, and inappropriate diagnoses and treatments including a wrong diagnosis have been performed.

SUMMARY OF THE INVENTION

Technical Problem

[0007] The cause of the difficulty of the problem is that cystoscope observations are frequently avoided in some regions where cystoscope findings are not always required for the diagnosis of interstitial cystitis. In this case, it may be difficult to confirm Hunner lesions with accuracy, so that potential patients may be missed as described above. Even if cystoscope observations are conducted, doctors with insufficient knowledge may miss potential patients. Moreover, cystoscope observations are mostly conducted on patients who have felt bladder abnormalities. Thus, just a few opportunities of observations on normal bladders are provided and only a few cystoscope images of normal bladders are accumulated. Furthermore, some doctors do not have knowledge about how to distinguish normal bladders from abnormal bladders free of Hunner lesions. Such circumstances cause a vicious cycle of difficulty in the definition of global standards and criteria.

[0008] However, regardless of the knowledge and skill of doctors, if a versatile technique capable of accurately and quickly identifying a Hunner lesion of a patient is provided and if a technique capable of properly recognizing a normal bladder is provided, remarkable progress is made in all of an accurate diagnosis of interstitial cystitis, the rescue of interstitial cystitis patients, and international consensus building.

Solution to Problem

[0009] In order to solve the problem, the present invention includes a method for generating a learning model, the method including: acquiring, as teaching data, endoscope image data on a Hunner lesion in a bladder; and generating the learning model by using the teaching data such that a bladder endoscope image serves as an input and the position indication of a Hunner lesion in the bladder endoscope image serves as an output.

[0010] Furthermore, the present invention includes a program that causes a computer to perform processing for acquiring endoscope image data on a Hunner lesion in a bladder, inputting a target bladder endoscope image to a learning model in which a bladder endoscope image serves as an input and position-indication data on a Hunner lesion in an endoscope image serves as an output, and outputting the position indication of the Hunner lesion.

[0011] Furthermore, the present invention includes a learned model that uses a bladder endoscope image acquired by using a bladder endoscope system, the learned model including an input layer that receives the bladder endoscope image, an output layer in which position indication data on a Hunner lesion in the endoscope image serves as an output, and an intermediate layer having a parameter learned by using teaching data in which endoscope image data on the Hunner lesion in a bladder serves as an input and position indication data on the Hunner lesion in the bladder image serves as an output, the learned model causing a computer to function to input a target bladder endoscope image to the input layer, perform an operation in the intermediate layer, and output the position indication data on the Hunner lesion in the image.

[0012] Moreover, the learning-model generating method, the program, the learned model preferably include, as teaching data, at least one of endoscope image data on air in a bladder, endoscope image data on a normal bladder, and endoscope image data on abnormal bladders free of Hunner lesions.

[0013] Furthermore, the image data preferably includes both of an image of narrow band imaging and an image of white light imaging.

[0014] Moreover, process of determination whether a bladder is normal or not and outputting is preferably enabled, and a program or a learned model is preferably installed in the controller of a bladder endoscope.

[0015] The program and the learned model of the present invention can be implemented by using known configurations, for example, a controller or a server including a CPU, a GPU, a ROM, a RAM, and a communication interface. Moreover, the program and the learned model can be configured as cloud systems. Furthermore, the present invention preferably includes means that causes display means such as a display to indicate and display the position of an estimated Hunner lesion by visually recognizable means such as framing or coloring. Moreover, the present invention may be used as a system to be used independently of an endoscope or may be used in the controller of a bladder endoscope system in real time during an observation in a bladder.

[0016] Furthermore, a deep learning model is used in the present invention. Typically, deep learning using a neural network is used, and a convolutional neural network is preferably used. When an image is inputted, a convolutional neural network acts as estimating means for estimating the position of a Hunner lesion. The estimating means is not limited thereto unless the effect of the present invention is disabled.

[0017] A deep learning model includes a large number of internal parameters. The internal parameters are adjusted to obtain, contrary to input data, an output result closest to teaching data. This adjustment is generally called "learning." In order to generate a high-performance model, the amount and quality of teaching data (a set of input data and teaching data) used for learning is important in addition to a model structure and a learning method.

[0018] Teaching data in the present invention is an endoscope image of a Hunner lesion in a bladder. A model capable of indicating the Hunner lesion is generated by indicating and learning the Hunner lesion. As a result of study, it was found that air (bubbles) in a bladder may be identified as a Hunner lesion or a Hunner lesion may be indicated in a normal bladder (it is assumed that a shadow of wrinkles or a height difference in a normal bladder may affect the indication). Thus, in order to prevent these factors from being identified as Hunner lesions, air (bubbles) was learned as air (bubbles). Since a mucosal condition of a normal bladder is different from a bladder condition of interstitial cystitis regardless of the presence or absence of a Hunner lesion, images of abnormal bladders free of Hunner lesions were learned in addition to images of normal bladders.

[0019] In the present invention, normal bladders are learned to effectively eliminate a determination rate of false positives about normal bladders. Moreover, images of abnormal bladders free of Hunner lesions are learned to effectively avoid the determination of false positives about abnormal bladders free of Hunner lesions. Furthermore, if a model is generated to output a normal bladder as a normal bladder, a configuration for determining and indicating, as an abnormal bladder, an abnormal bladder free of Hunner lesions can be achieved.

[0020] In order to obtain algorithms with high accuracy, it is necessary to learn a large number of Hunner lesion patterns. However, only a small number of bladder endoscope images of interstitial cystitis patients has been globally accumulated. Tomohiro Ueda, one of the inventors, has accumulated the largest number of bladder endoscope images of interstitial cystitis patients (and normal bladder images and images of abnormal bladders free of Hunner lesions) in the world. Thus, a wide variety of Hunner lesion images has been accumulated, allowing learning of images of sufficient types and quality for generating a model. Moreover, images of both of narrow band imaging (NBI) and white light imaging (WLI) are learned in the present invention, so that the model is usable for images of NBI and WLI. In narrow band imaging, narrowband light of two wavelengths of blue (wavelength from 390 nm to 445) and green (wavelength of 530 nm to 550 nm) is emitted, and a microscopic vessel image is outputted with an enhanced contrast. Blue light indicates the presence or absence of a neovascular on a mucous membrane while green light indicates the presence or absence of a vessel deep under a mucous membrane. White light imaging is an observation using illumination light of primary colors of blue, green, and red from the tip of an endoscope. In actual diagnoses by doctors, lesions are more likely to be visually confirmed in narrow band imaging. However, it is assumed that the utilization rate of white light imaging is higher than that of narrow band imaging in the world including developing countries. In white light imaging, a lesion and a background look red, causing difficulty in diagnosis. The present invention is also applicable to white light imaging and thus is so versatile as to be useful for finding patients of interstitial cystitis and building an international consensus.

BRIEF DESCRIPTION OF DRAWINGS

[0021] FIG. **1** shows examples of WLI and NBI images of a normal condition, bubbles, and a Hunner lesion;

[0022] FIG. **2** shows a score example of an IoU;

[0023] FIG. **3** is a conceptual diagram of TP, FP, and FN;

[0024] FIG. **4** shows an example of the NBI image prediction result of a detection model (Cascade R-CNN);

[0025] FIG. **5** shows an example of the NBI image prediction results of the detection model and a segmentation model;

[0026] FIG. **6** shows an example of the WLI image prediction results of the detection model and the segmentation model; and

[0027] FIG. **7** shows a detection result example of NBI normal bladder images in the detection model and the segmentation model.

DESCRIPTION OF EMBODIMENTS

Dataset

[0028] Based on moving images captured by a bladder endoscope, correct information is added (annotation) to the moving images in the following steps:

[0029] 1. A candidate image is extracted every ten frames from all frames, and a Hunner-lesion candidate image is selected;

[0030] 2. Correct information is added to the selected image; and

[0031] 3. In frames around the image to which the correct information has been added, the correct information is added to similar images.

[0032] Data to which the correct information has been added was divided into NBI and WLI to produce a database of still images. In an extracted image, a black area outside an endoscope image was erased by trimming. This processing obtains a pixel size of about 1000×900 pixels. Moreover, an annotation at the position of a Hunner lesion was made by software called Label me.

[0033] The number of moving images

TABLE 1

Dataset	The number of moving images
Year 2016	1940
Year 2017	1952
Year 2018	2005
Year 2019	2259
Year 2020	64

[0034] Still-image database configuration

TABLE 2

	NBI The number of still images	WLI The number of still images
Normal image	672	726
Hunner lesion	2758	1591
Bubbles	573	17

*Normal images include images of normal bladders and abnormal bladders free of Hunner lesions but do not include images having Hunner lesions.

[0035] Bubbles include images of normal bladders and images having Hunner lesions.

[0036] FIG. **1** shows examples of WLI and NBI images of a normal condition, bubbles, and a Hunner lesion.

[0037] The image examples of bubbles in FIG. **1** are image examples of abnormal bladders free of Hunner lesions. Original images are all color images that clarify a difference in visibility between WLI and NBI, facilitating understanding of an advantage of NBI.

Model

[0038] An experiment was conducted by using a detection model and a segmentation model. The detection model is a model for estimating a rectangular area including a Hunner lesion area. The position and size of the rectangular area and the lesion confidence factor of the rectangle. The segmentation model is a model for outputting a lesion confidence factor for each pixel. A Hunner lesion area is estimated as well as the shape of the area.

[0039] In the experiment, models of high performance for a dataset of general images (COCO, CITYSCOPES) were used as follows:

[0040] Detection model: Cascade R-CNN;

[0041] Segmentation model: Cascade Mask R-CNN; and

[0042] Segmentation model: OCNet.

[0043] The three models were learned with data of NBI and WLI, and six models were created in total.

Experiment Setting and Result

[0044] In the experiment, the dataset was randomly divided into learning data of 85% and test data of 15% five times, and learning and evaluation were performed five times. The data was divided for each case. Tables 3 and 4 indicate the number of images and the number of cases in NBI and WLI datasets.

[0045] The number of images and the number of cases in NBI dataset

TABLE 3

	Learning data		Test data	
Divided dataset number	The number of images	The number of cases	The number of images	The number of cases
1	3478	122	514	20
2	3478	122	514	20
3	3365	122	627	20
4	3361	122	631	20
5	3439	122	553	20

[0046] The number of images and the number of cases in WLI dataset

TABLE 4

	Learning data		Test data	
Divided dataset number	The number of images	The number of cases	The number of images	The number of cases
1	1909	95	329	15
2	1969	95	269	15
3	1952	95	286	15
4	1773	95	465	15
5	1875	95	363	15

[0047] Three models (Cascade R-CNN, Cascade Mask R-CNN, OCNET) were learned for each image type and each divided dataset, and the performance of each model was evaluated based on the sensitivity and the positive prediction value of each Hunner lesion area. The sensitivity and the positive prediction value (PPV) are expressed as follows:

Sensitivity=#TP/(#TP+#FN) PPV=#TP/(#TP+#FP) where #TP is the number of true positives, #FN is the number of false negatives, and #FP is the number of false negatives.

[0048] A method for determining a true positive (TP), a false negative (FN), and a false positive for each Hunner lesion area will be described below. First, the degree of overlapping of a predicted area and a correct area is calculated by an IoU (Intersection over Union). The IoU is the ratio of the number of duplicate pixels in the predicted area and the correct area relative to the number of pixels in the union area of the predicted area and the correct area. If the two areas do not overlap each other at all, the IoU is 0, whereas if the two areas completely agree with each other, the IoU is 1. FIG. **2** shows a score example of the IoU for rectangular areas. Dotted lines indicate correct areas, and solid lines indicate predicted areas.

[0049] In the present example, TP, FN, and FP were defined as follows:

[0050] TP=a correct area where the IoU exceeds 0.3 relative to all predicted areas, each including at least one duplicate pixel;

[0051] FN=a correct area where the IoU is not larger than 0.3 relative to all predicted areas, each including at least one duplicate pixel; and

[0052] FP=a predicted area where the IoU is not larger than 0.1 relative to the correct area.

[0053] As described above, Cascade R-CNN, a detection model, is evaluated with rectangular regions. Cascade Mask R-CNN and OCNET, segmentation models, are evaluated in consideration of area shapes. The correct areas and the predicted areas are provided. As shown in FIG. **3**, the upper correct area (left) and the upper predicted area hardly overlap each other and thus are denoted as FN and FP. The lower correct area (center) sufficiently overlapping multiple predicted areas is denoted as TP.

[0054] FIG. **3** shows a conceptual diagram of the TP, FP, and FN.

[0055] Tables 5 to 8 below show the evaluation results of each model. FIGS. **4** to **7** show the NBI image prediction results of each model. FIG. **6** shows a detection result example of NBI normal bladder images in the detection model and the segmentation model. The original images of FIGS. **4** to **7** are all color photos.

[0056] Table 5: the performance of the detection model (Cascade R-CNN) evaluated in an NBI image

[0057] Table 6: the performance of the segmentation model evaluated in an NBI image

[0058] Table 7: the performance of the detection model (Cascade R-CNN) evaluated in a WLI image

[0059] Table 8: the performance of the segmentation model evaluated in a WLI image

[0060] The performance of the detection model (Cascade R-CNN) evaluated in an NBI image

TABLE 5

Divided	Evaluation in all predicted areas					Evaluation in predicted areas having a confidence factor of 50% or more				
dataset number	TP	FP	FN	PPV	Sensitivity	TP	FP	FN	PPV	Sensitivity
1	359	350	145	0.51	0.71	324	136	180	0.70	0.64
2	308	608	208	0.34	0.60	256	228	260	0.53	0.5

TABLE 5-continued

Divided	Evaluation in all predicted areas					Evaluation in predicted areas having a confidence factor of 50% or more				
dataset number	TP	FP	FN	PPV	Sensitivity	TP	FP	FN	PPV	Sensitivity
3	524	689	327	0.43	0.61	424	271	427	0.61	0.5
4	464	598	205	0.44	0.69	405	250	264	0.62	0.6
5	486	844	157	0.36	0.76	432	432	211	0.5	0.67
Average				0.41 ± 0.068	0.67 ± 0.068				0.59 ± 0.079	0.58 ± 0.078

[0061] The performance of the segmentation model evaluated in an NBI image

TABLE 6

Divided dataset	Cascade Mask R-CNN		OCNET	
number	PPV	Sensitivity	PPV	Sensitivity
1	0.67	0.71	0.84	0.57
2	0.49	0.64	0.62	0.38
3	0.63	0.68	0.59	0.40
4	0.5	0.65	0.81	0.66
5	0.38	0.66	0.55	0.44
Average	0.53 ± 0.116	0.67 ± 0.027	0.68 ± 0.133	0.49 ± 0.120

*Evaluation with all prediction pixels (pixels with a confidence factor other than 0%) having reactions from the model

[0062] The performance of the detection model (Cascade R-CNN) evaluated in a WLI image

TABLE 7

Divided	Evaluation in all predicted areas					Evaluation in predicted areas having confidence fact of 50% or more				
dataset number	TP	FP	FN	PPV	Sensitivity	TP	FP	FN	PPV	Sensitivity
1	190	133	36	0.59	0.84	179	59	47	0.75	0.79
2	241	150	26	0.62	0.90	225	74	42	0.75	0.84
3	251	195	90	0.56	0.74	218	109	123	0.66	0.63
4	470	245	61	0.66	0.88	418	83	113	0.83	0.79
5	337	241	100	0.58	0.77	312	130	125	0.71	0.71
Average				0.60 ± 0.039	0.83 ± 0.069				0.74 ± 0.062	0.75 ± 0.083

[0063] The performance of the segmentation model evaluated in a WLI image

TABLE 8

Divided dataset	Cascade Mask R-CNN		OCNET	
number	PPV	Sensitivity	PPV	Sensitivity
1	0.45	0.91	0.78	0.54
2	0.56	0.98	0.87	0.64
3	0.45	0.90	0.76	0.47
4	0.56	0.94	0.80	0.79
5	0.50	0.91	0.63	0.38
Average	0.50 ± 0.055	0.93 ± 0.032	0.76 ± 0.087	0.56 ± 0.158

*Evaluation with all prediction pixels (pixels with a confidence factor other than 0%) having reactions from the model

[0064] FIG. **4** shows an example of the NBI image prediction result of the detection model (Cascade R-CNN).

[0065] All predicted areas with a confidence factor other than 0% are displayed. Dotted lines (green in the original images) indicate correct areas, and solid lines (red in the original images) indicate predicted areas, which sufficiently indicates a Hunner lesion.

[0066] FIG. **5** shows an example of the NBI image prediction results of the detection model and the segmentation model.

[0067] Rectangular outputs are displayed with confidence factors in addition to area specifications. An upper left image, an upper central image, and an upper right image sequentially indicate Hunner lesions with confidence factors of 0.78 (left), 0.9 (center), and 0.97 (right). A lower left image, a lower central image, and a lower right image sequentially indicate a Hunner lesion with a confidence factor of 0.33 and bubbles with a confidence factor of 0.79 (left), bubbles with a confidence factor of 0.97 (center), and a Hunner lesion with a confidence factor of 0.98 and a confidence factor of 0.4. In the present example, bubbles are indicated as bubbles in output display, so that the indication is successfully distinct from that of a Hunner lesion. In the original image, the correct area is indicated in green.

[0068] FIG. **6** shows an example of the WLI image prediction results of the detection model and the segmentation model.

[0069] Rectangular outputs are displayed with confidence factors in addition to area specifications. From the left to the right, a Hunner lesion is indicated with confidence factors of 0.96 and 0.99 (left), 0.97 (center), and 0.997 (right). This successfully provides a sufficient indication of a Hunner lesion. In the original image, the correct area is indicated in green.

[0070] FIG. **7** shows a detection result example of NBI normal bladder images in the detection model and the segmentation model. In the normal bladder, any Hunner lesions have not been indicated. Determination of a false positive has been avoided even in a bladder having a different image appearance.

[0071] As described above, a learned model applicable to images of narrow band imaging and white light imaging can be formed. Moreover, bubbles can be indicated. According to the present invention, an opportunity can be provided to accurately and quickly identify a Hunner lesion in images of narrow band imaging and white light imaging regardless of the knowledge and skill of a doctor. Furthermore, determination of a false positive is avoided even if a height difference is made or a red phase is caused by a shadow or the like in a normal bladder. Consequently, the present invention contributes to the progress of an accurate diagnosis of interstitial cystitis, the rescue of interstitial cystitis patients, and international consensus building.

What is claimed is:

1. A method for generating a learning model, the method comprising:

acquiring, as teaching data, endoscope image data on a Hunner lesion in a bladder, and

generating the learning model by using the teaching data such that a bladder endoscope image serves as an input and position indication of a Hunner lesion in the bladder endoscope image serves as an output.

2. The method for generating a learning model according to claim **1**, wherein endoscope image data on air in a bladder is further included as teaching data.

3. The method for generating a learning model according to claim **1**, wherein the endoscope image data in the teaching data includes both of an image of narrow band imaging and an image of white light imaging.

4. A program that causes a computer to perform processing for acquiring endoscope image data on a Hunner lesion in a bladder,

inputting a target bladder endoscope image to a learning model in which a bladder endoscope image serves as an input and position-indication data on a Hunner lesion in an endoscope image serves as an output, and outputting position indication of the Hunner lesion.

5. The program according to claim **4**, wherein the endoscope image data in teaching data includes both of an image of narrow band imaging and an image of white light imaging.

6. The program according to claim **4**, wherein endoscope image data on air in a bladder is further included as teaching data.

7. A controller of a bladder endoscope, wherein the program according to claim **4** is recorded.

* * * * *